

Evaluation of Single Heated Channel and Subchannel Modelling on a Nuclear Once Through Steam Generator (OTSG)

Hamedani A.¹, Noori-Kalkhoran O.* and Shirani A.S.¹

*Author for correspondence

Nuclear Science and Technology Research Institute (NSTRI)
Tehran, IRAN

E-mail: onoori@aeoi.org.ir

¹Faculty of Engineering, Shahid Beheshti University, Tehran, IRAN

ABSTRACT

Steam generator is one of the most important components of pressurized-water reactor. This component plays the role of heat transfer and pressure boundary between primary and secondary side fluids. The Once Through Steam Generator (OTSG) is an essential component of the integrated nuclear power system. In this paper steady state analysis of primary and secondary fluids in the Integral Economizer Once Through Steam Generator (IEOTSG) have been presented by Single Heated Channel (SHC) and subchannel modelling. Models have been programmed by MATLAB and FORTRAN. First, SHC model has been used for this purpose (changes are considered only in the axial direction in this model). Second, subchannel approach that considers changes in the axial and also radial directions has been applied. Results have been compared with Babcock and Wilcox (B&W) 19-tube once through steam generator experimental data. Thermal-hydraulic profiles have been presented for steam generator using both of models. Accuracy and simplicity of SHC model and importance of localization of thermal-hydraulic profiles in subchannel approach has been proved.

INTRODUCTION

Steam generator is a heat exchanger which produces steam that is needed for steam turbine in nuclear power plant. It is a barrier to separate the primary and secondary coolant sides. Heat that is generated in the reactor core is carried by primary fluid which transfers this heat to the secondary fluid through indirect contact in the steam generator. Problems due to the fatigue are usually occurred in 10-15 years of initial plant performance and reliability of the steam generator must be considered continuously to present reliable and practical solutions in order to deal with the different problems. Thermal-hydraulic analysis of steam generator provides basic necessary information to elevate the performance, erosion, corrosion and failure caused by vibrations applied by flow field and detection and obviation of obstructions, etc[1]. Given the importance of these, several studies have been done in recent years to evaluate the thermal-hydraulic behavior of steam generator. A compressible model with fixed boundary was applied to study the thermal-hydraulic characteristics of an annular tube once through steam generator[2]. Jingyan et al. have presented a mathematical model for OTSG with concentric annuli tube based on conservation equations[3]. Numerical investigation of thermal-hydraulic characteristics in OTSG have been done by using a coupled primary and secondary side heat transfer in

several studies[4, 5]. Some different models have been used to model steam generator primary and secondary sides [6-9]. Almost in all these models each of primary and secondary sides are treated as a single flow channel. In other words behavior and characteristics of primary and secondary fluids in all tubes and all regions are considered equal in radial direction. In this study thermal-hydraulic parameters of primary and secondary fluids are modeled with Single Heated Channel (steam generator has been considered as a channel in each of the two sides) and subchannel (steam generator has been considered as several different channels in each of two sides that mass and momentum can be exchanged between channels) models. Models have been programmed by MATLAB and FORTRAN languages. First subchannel model has been validated by modeling General Electric 9-fuel rod core, presented in THERMIT[10] code and comprising the results. Both of models have been applied for B&W 19-tube once through steam generator and results have been compared with experimental results. The structure of B&W 19-tube OTSG have been shown in Figure 1 and 2 and flow specification are presented in Table 1.

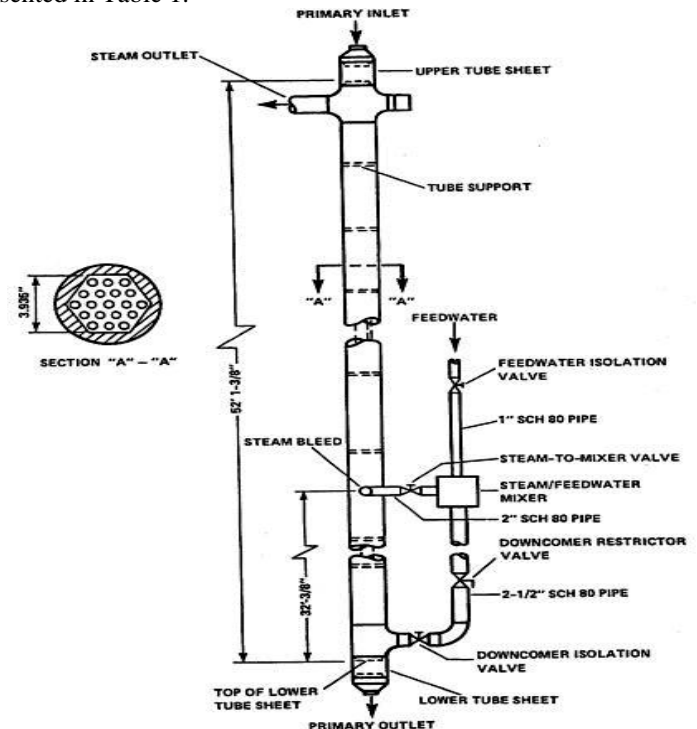


Figure 1 B&W 19-tube OTSG

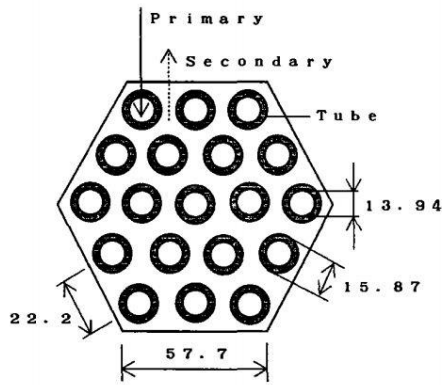


Figure 2B&W 19-tube OTSG cross section(Unit = mm)

Table 1 Flow Specifications and boundary conditions of B&W 19-tube OTSG

Primary fluid output temperature	300 °C
Primary fluid output velocity	5.6 m/s
Primary fluid pressure	15.3 MPa
Secondary fluid input temperature	251.7 °C
Secondary fluid input velocity	0.3 m/s
Secondary fluid pressure	7.4 MPa

NOMENCLATURE

A	Area
C_T	Parameter of modeling
D	Diameter
e	Switch function
$f(f_w)$	Friction factor coefficient
F	Axial mass flow rate
g	Earth's gravity acceleration
G	Mass flux
h^+	Dynamic enthalpy
h	Enthalpy
k (k_{li})	Local loss coefficient
K_G	Overall loss coefficient
l	Subchannel-to-subchannel centroid distance
p	Pressure
$P_h(P_H)$	perimeter
q	Heat Flux
s	Gap size
S	Switch matrix
T	Temperature
U	velocity component in the axial direction
U^*	Average axial velocity component
V	velocity component in the lateral direction
V'	Reference Velocity
w	Lateral mass flow rate
W'	Turbulent mixing
x	Thermodynamic quality
x_c	Critical quality

Greek Letters

α	Void fraction
β	Turbulent mixing coefficient for a gap with reference cent centroid distance
$v(V')$	Specific volume
ρ	Density
ρ^+	Dynamic density
v	Phase velocity
τ	Viscous shear stress
Φ_{ip}	Two phase friction multiplier
ϕ_{im}	Fraction of tube total perimeter that actually faces the subchannel

Subscripts

m	Mixture
l	liquid
v	vapour

OTSG DESCRIPTION

Reactor coolant that carries thermal energy which is produced in the core enters the OTSG from the top and flows downward inside the tubes. Secondary fluid enters from bottom and flows upward in the shell side. Heat from primary side transfers to the secondary side through tube walls and secondary fluid gets warm and warmer. Secondary fluid is in subcooled state at the entrance. As the heat is added four heat transfer regimes are considered respectively[11]:

subcooled water : ($T_{bulk} < T_{sat}, T_{wall} < T_{sat}$),

subcooled boiling : ($T_{bulk} < T_{sat}, T_{wall} > T_{sat}$),

saturated boiling : ($T_{bulk} = T_{sat}, quality(x) < 1.0$) and

superheated vapor : ($quality(x) > 1.0$).

These regions are shown in Figure 3. Heat transfer coefficients for each region are different. Dittus-Boelter equation for single phase flow and chen's correlations for two phase flow are used [11]. Steady state analysis is presented and thermal equilibrium homogeneous model is considered for two phase flow. Primary fluid remains single phase in the steam generator.

MODELING

SINGLE HEATED CHANNEL METHOD (SHC)

In this method, given geometry is considered as a channel that has same equivalent parameters including hydraulic diameter, heated area and etc. Basic equations for this method are obtained from conservation equations. Mass, momentum and energy equations for heating channel with upward flow are presented below[12]:

Mass Balance :

$$\frac{\partial \rho_m}{\partial t} + \frac{\partial}{\partial z}(G_m) = 0 \quad (1)$$

Momentum Balance :

$$\frac{\partial G_m}{\partial t} + \frac{\partial}{\partial z} \left(\frac{G_m^2}{\rho_m^+} \right) = -\frac{\partial p}{\partial z} - \frac{f G_m |G_m|}{2 D_e \rho_m} - \rho_m g \cos \theta \quad (2)$$

Energy Balance :

$$\frac{\partial}{\partial t} (\rho_m h_m) + \frac{\partial}{\partial z} (G_m h_m^+) = \frac{q'' P_h}{A_z} + \frac{\partial p}{\partial t} + \frac{G_m}{\rho_m} \left[f \frac{G_m |G_m|}{2 D_e \rho_m} + \frac{\partial p}{\partial z} \right] \quad (3)$$

Parameters were defined as below:

$$\text{Mixture density: } \rho_m = \{ \rho_v \alpha \} + \{ \rho_l (1 - \alpha) \} \quad (4)$$

Mass flux (average mass flow rate per unit flow area):

$$G_m = \{ \rho_v \alpha v_{vz} \} + \{ \rho_l (1 - \alpha) v_{lz} \} \quad (5)$$

Dynamic (or mixing cup) density:

$$\frac{1}{\rho_m^+} \equiv \frac{1}{G_m^2} \{ \rho_v \alpha v_{vz}^2 + \rho_l (1 - \alpha) v_{lz}^2 \} \quad (6)$$

Static mixture enthalpy (averaged over the flow area):

$$h_m = \{ \rho_v \alpha h_v + \rho_l (1 - \alpha) h_l \} / \rho_m \quad (7)$$

Dynamic mixture enthalpy:

$$h_m^+ = \{ \rho_v \alpha h_v v_{vz} + \rho_l (1 - \alpha) h_l v_{lz} \} / G_m \quad (8)$$

In derivation of these equations some assumption were applied:

- Flow direction is upward (for downward and cooling flow just the sign of terms will be changed)
- Coolant equations are radially averaged.
- Flow area is considered constant.
- Same pressure for liquid and steam phase ($P_v = P_l = P$)
- Pressure is uniform in the flow area.

With consideration of thermal equilibrium homogenous two phase flow, some parameters of presented equations will be changed:

$$\rho_m^+ = G_m^2 / (G_v + G_l) v_m = \rho_m \quad (9)$$

$$h_m^+ = h_m \quad (10)$$

Using equations (1), (2), (3) and assumptions that have been noted, final equations of SHC method for two phase flow will be presented as :

$$h_m(z) = h_{m_{in}} + \frac{q}{\dot{m}} + \frac{1}{\rho_m} [p(z) - p_{in}] + f \frac{G_m |G_m|}{2 \rho_m D_e} \quad (11)$$

$$\Delta p = \Delta p_{acc} + \Delta p_{gravity} + \Delta p_{friction} + \Delta p_{form} \quad (12)$$

$$\Delta p_{acc} = \left(\frac{G_m^2}{\rho_m^+} \right)_{z+1} - \left(\frac{G_m^2}{\rho_m^+} \right)_z \quad (13)$$

$$\Delta p_{gravity} = \int_z^{z+1} \rho_m g dz \quad (14)$$

$$\Delta p_{friction} = \phi_{sp}^2 \frac{f_l G_m |G_m|}{2 D_e \rho_l} \Delta z \quad (15)$$

$$\Delta p_{form} = \sum_i \left(\phi_{sp}^2 k \frac{G_m |G_m|}{2 \rho_l} \right)_i \quad (16)$$

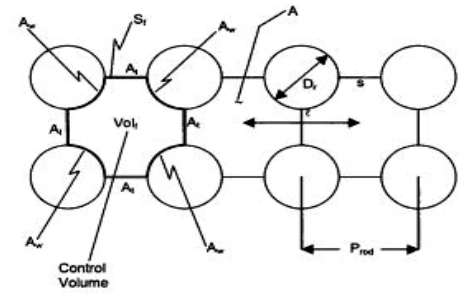
$$T_{z+1} = T_z + \frac{q}{\dot{m} C_p} + \frac{1}{C_p \rho_m} \left((p_{z+1} - p_z) + f \frac{G_m |G_m|}{2 \rho_m D_e} (\Delta z) \right) \quad (16)$$

$$p_i - p_{i+1} = \frac{f G_m |G_m|}{2 D_e \rho_l} (Z_{i+1} - Z_i) + \Delta p_{form} + \rho_l g (Z_{i+1} - Z_i) \quad (17)$$

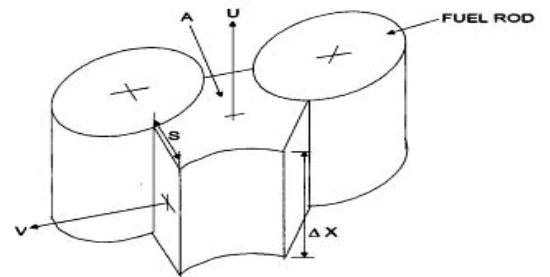
for single phase flow.

SUBCHANNEL APPROACH

In this method, flow area is divided to the number of smaller channels called subchannels and a suppositional boundary is considered between adjacent subchannels (Gaps). Adjacent subchannels that are in the two side of a gap, exchange mass, momentum and energy through these gaps. Because of existence of these gaps between subchannels the lateral flow is important in this method, though in all the equations derived for subchannel approach, this flow is considered and also beside the axial momentum equation, lateral momentum equation is solved. The basic equations for deriving subchannel equations are Navier-Stokes equations [13] that have been presented below. Control volume that is used in deriving the equations is shown in figure 3 for square array and triangular array.



(a) Plane View - Square Array



(b) Perspective View - Triangular Array

Figure 3 Subchannel geometry

Mass Balance :

The mass balance of Navier-Stokes equation is:

$$\frac{\partial}{\partial t} \int_{Vol_j} \rho dV + \int_{S_A} \rho (\vec{V} \cdot \vec{n}) dA = 0 \quad (19)$$

Result of applying this equation to the control-volume shown in Figure 4, is:

$$\frac{\partial}{\partial t} \int_{Vol_f} \rho d\bar{V} + \int_A \rho (\vec{V} \cdot \vec{n}) d\bar{A} + \int_{s \Delta x} \rho (\vec{V} \cdot \vec{n}) d\bar{A} = 0 \quad (20)$$

Performing the integrations in the equation gives:

$$A \Delta x \frac{\partial}{\partial t} \rho + [(\rho UA)_{x+\Delta x} - (\rho UA)_x] + \sum_{k \in i} e_{ik} \rho V_s \Delta x = 0 \quad (21)$$

Where the summation in the last term on the left-hand side is over all transverse gaps, k, associated with the control volume (Vol_f). Dividing equation (21) by Δx , and taking the limit as Δx approaches zero gives:

$$A \frac{\partial}{\partial t} \rho + \frac{\partial}{\partial x} F + \sum_{k \in i} e_{ik} w = 0 \quad (22)$$

Where F is the mass flow rate in the axial primary direction:

$$F = \rho UA \quad (23)$$

And w is the mass flow per unit length in the lateral direction through the gaps:

$$w = \rho V_s \quad (24)$$

Geometry variations and non-uniform changes in fluid density can establish transverse pressure gradients between subchannels. Geometry variations include every possibility that design features introduce variations in the subchannel flow area or the axial pressure gradient. The fluid density is most greatly affected by the presence of boiling. Variations in the radial and axial heat flux distribution can result in boiling onset in some subchannels while the fluid in adjacent subchannels remains in the subcooled liquid state. After boiling starts, the pressure gradient in the boiling subchannel will differ from that in the non-boiling subchannels. The resulting difference will affect the cross flow between the subchannels. The axial and lateral flow rates are defined in terms of average fluxes. At last finite-difference form of the mass conservation for axial level J is:

$$A_J \frac{\Delta x_J}{\Delta t} (\rho^{n+1} - \rho^n) + F_J^{n+1} - F_{J-1}^{n+1} + \Delta x_J \sum_{k \in i} e_{ik} w_J^{n+1} = 0 \quad (25)$$

One of the most important points in subchannel approach is that the connection and exchange between subchannels through the gaps, implies that the solving of conservation equations must be linked and because of that, subchannel approach is solved in the matrix form. Thus the vector form of the finite difference equation would be useful:

$$A_J \left\{ \frac{\rho_J^{n+1} - \rho_J^n}{\Delta t} \right\} + \frac{F_J^{n+1} - F_{J-1}^{n+1}}{\Delta x_J} = -[S]^T \{w_J^{n+1}\} \quad (26)$$

Where $[S]^T w_J^{n+1} = \sum_{k \in i} e_{ik} w_J^{n+1}$, which [S] is matrix with switch elements (e_{ik}).

Momentum Balance :

The momentum balance equation as the basis of subchannel momentum equation is :

$$\frac{\partial}{\partial t} \int_{Vol_f} \rho \vec{V} d\bar{V} + \int_{s_x} \rho \vec{V} (\vec{V} \cdot \vec{n}) d\bar{A} = - \int_{A+A_f} P \vec{n} d\bar{A} + \int_{A+A_f} (\vec{\tau} \cdot \vec{n}) d\bar{A} + \int_{Vol_f} \rho \vec{g} d\bar{V}$$

In applying equation (27) to the control volume (Figure 3), some assumptions simplify terms of this equation :

- There is no fluid flow across the walls of tubes, so second term of the left-hand side is of interest only on the fluid surfaces.
- The pressure gradient, first term on the right hand side, contributes both at the solid walls and within the fluid.
- The viscous shear stresses are not resolved within the fluid in the axial direction so the second term on the right-hand side is presented by the stresses due to the solid tube walls and viscous stresses within the fluid at the interface between subchannels.

Using these assumptions the overall momentum equation will be:

$$\frac{\partial}{\partial t} \int_{Vol_f} \rho \vec{V} d\bar{V} + \int_{A+A_f} \rho \vec{V} (\vec{V} \cdot \vec{n}) d\bar{A} = - \int_{A+A_f} P \vec{n} d\bar{A} - \int_{A_w} P \vec{n} d\bar{A} + \int_{A+A_f} (\vec{\tau} \cdot \vec{n}) d\bar{A} + \int_{A_w} (\vec{\tau} \cdot \vec{n}) d\bar{A} + \int_{Vol_f} \rho \vec{g} d\bar{V} \quad (28)$$

Axial Momentum Balance :

For axial flow, the definition of each term in equation (28) is:

$$\text{Momentum flux:} \int_{A+A_f} \rho \vec{V} (\vec{V} \cdot \vec{n}) d\bar{A} = [(\rho U^2 A)_{x+\Delta x} - (\rho U^2 A)_x] + \sum_{k \in i} e_{ik} \rho UV_s \quad (29)$$

The wall and fluid pressure forces:

$$- \int_{A+A_f} P \vec{n} d\bar{A} - \int_{A_w} P \vec{n} d\bar{A} = -A [P_{x+\Delta x} - P_x] \quad (30)$$

The viscous shear stresses acting on the tube walls:

$$\int_{A_w} (\vec{\tau} \cdot \vec{n}) d\bar{A} = -\frac{1}{2} \left(\frac{f_w}{D_{hy}} \Delta x + K_{ll} \right) \rho U |U| A, f_w = 4f' \quad (31)$$

The viscous stresses acting within the fluid:

$$\int_{A+A_f} (\vec{\tau} \cdot \vec{n}) d\bar{A} = -C_T \Delta x \sum_{k \in i} w' (\Delta U) \quad (32)$$

Volumetric body force:

$$\int_{Vol_f} \rho \vec{g} d\bar{V} = -A \rho \Delta x g \cos \theta \quad (33)$$

Parameters of these equations are defined as presented below:

The friction factor, f' , represents the wall shear stress due to the flow parallel to the tubes. K_{ll} , represents the effects of local changes in the flow channel geometry. w' is the turbulent cross flow per unit length at the subchannel interface. ΔU is the axial velocity difference between the subchannel of interest and an adjacent one. With substituting given terms in equation (28), the axial momentum equation is:

$$A \frac{\partial}{\partial t} \rho U + \frac{\partial}{\partial x} \rho U^2 A + \sum_{k \in i} e_{ik} \rho U V_s = -A \frac{\partial P}{\partial x} - \frac{1}{2} \left(\frac{f_w}{D_{hy}} + K' \right) \rho U |U| A - C_T \sum_{k \in i} w' (\Delta U) - A \rho g \cos \theta \quad (34)$$

The finite difference form of this equation is:

$$\left\{ \frac{1}{A_j} \frac{F_j^{n+1} - F_j^n}{\Delta t} \right\} - \left\{ 2U_j^{n+1} \frac{\rho_j^{n+1} - \rho_j^n}{\Delta t} \right\} + \left\{ \frac{P_j^{n+1} - P_{j-1}^{n+1}}{\Delta x_j} \right\} = \{ \alpha'_j \} + [A_j]^{-1} \left[[2U_j] [S]^T - [S]^T [U_j^*] \right] \{ w_j^{n+1} \} \quad (35)$$

$$\{ \alpha'_j \} = - \left\{ K_j (F_j^{n+1})^2 \right\} - \{ f_j \} \quad (36)$$

$$K_j = \frac{K'_f}{\Delta x_j} + \frac{1}{A_j} \frac{A_j}{\Delta x_j} = \frac{1}{2} \left[\frac{f_w}{D_{hy}} \frac{\rho}{\rho_l} \Phi_{ip}^2 + \frac{K_l}{\Delta x} \right] \left(\frac{1}{\rho_j A_j^2} \right) + \frac{1}{A_j} \frac{A_j}{\Delta x_j} \quad (37)$$

$$\{ f_j \} = \rho_j^{n+1} g \cos \theta \quad (38)$$

Lateral Momentum Balance:

For deriving lateral momentum equation, terms of equation (28) are rewritten:

Pressure difference between the adjacent subchannels:

$$- \int_{A+A_j} P \bar{n} d\bar{A} - \int_{A_w} P \bar{n} d\bar{A} = -s \Delta x [P_{l+\Delta l} - P_l] \quad (39)$$

Fluid to wall momentum exchange due to viscosity at tube wall:

$$\int_{A_w} \bar{\tau} \bar{n} d\bar{A} = -\frac{1}{2} K_G \rho V |V| s \Delta x \quad (40)$$

$$\frac{\partial}{\partial t} \int_{V_{LM}} \rho V dV = ls \Delta x \frac{\partial}{\partial t} \rho V \quad (41)$$

Component of momentum flux in the axial direction:

$$\int_A \rho V (\bar{V} \cdot \bar{n}) d\bar{A} = [(\rho V U)_{x+\Delta x} - (\rho V U)_x] ls \quad (42)$$

Substituting these terms in equation (28) and dividing by Δx gives the lateral momentum, equation:

$$s \frac{\partial}{\partial t} \rho V + s \frac{\partial}{\partial x} \rho V U = \frac{s}{l} [P_{l+\Delta l} - P_l] - \frac{1}{2} K_G \rho V |V| \frac{s}{l} \quad (43)$$

The finite difference form of this equation is:

$$\left\{ \frac{w_j^{n+1} - w_j^n}{\Delta t} \right\} + \left\{ \frac{U_j^{*n+1} w_j^{n+1} - U_{j-1}^{*n+1} w_{j-1}^{n+1}}{\Delta x_j} \right\} + \left(\frac{s}{l} \right) \{ C_j w_j^{n+1} \} = \left(\frac{s}{l} \right) [S] \{ P_{j-1}^{n+1} \} \quad (44)$$

$$C_j = \frac{1}{2} K_G \frac{|w_j^{n+1}|}{s_j^2 \rho_j^{n+1}} \quad (45)$$

$$U_j^{*n+1} = \frac{1}{2} (U_{ii}^{n+1} + U_{jj}^{n+1}) \quad (46)$$

Energy Balance:

Navier-Stokes energy balance equation is in the form:

$$\frac{\partial}{\partial t} \int_{Vol_f} \rho h dV + \int_{S_A} \rho h (\bar{V} \cdot \bar{n}) d\bar{A} = - \int_{S_A} (q'' \cdot \bar{n}) d\bar{A} \quad (47)$$

Where:

$$\frac{\partial}{\partial t} \int_{Vol_f} \rho h dV = A \Delta x \frac{\partial}{\partial t} \rho h \quad (48)$$

Integration over the fluid flow surfaces bounding the control volume gives:

$$\int_{A+A_j} \rho h (\bar{V} \cdot \bar{n}) d\bar{A} = \int_A \rho h U d\bar{A} + \int_{s \Delta x} \rho h V d\bar{A} \quad (49)$$

$$= [(\rho h U A)_{x+\Delta x} + (\rho h U A)_x] + \Delta x \sum_{k \in i} e_{ik} (\rho h V) s$$

Energy exchange between the fluid and tube wall term is:

$$- \int_{A_w} (\bar{q} \cdot \bar{n}) d\bar{A} = \Delta x \sum_{m \in i} \phi_{im} P_H q_w'' \quad (50)$$

Energy transported by the turbulent fluctuations:

$$Q_m = \Delta x \sum_{k \in i} w' (\Delta h)$$

Where P_H is the total heated perimeter, ϕ_{im} , fraction of tube surface area that actually faces the control volume and q_w'' , the heat flux.

Substitution of these terms in equation (47) gives the energy equation for the subchannel approach:

$$A \frac{\partial}{\partial t} \rho h + \frac{\partial}{\partial x} \rho U h A + \sum_{k \in i} e_{ik} \rho V h s = \sum_{m \in i} \phi_{im} P_H q_w'' - \sum_{k \in i} w' (\Delta h)$$

And the finite difference form of this equation :

$$\left\{ \frac{1}{u_j''} \frac{h_j^{n+1} - h_j^n}{\Delta t} \right\} + \left\{ \frac{h_j^{n+1} - h_{j-1}^{n+1}}{\Delta x_j} \right\} = \quad (53)$$

$$[F_{j-1}^{n+1}]^{-1} \left\{ \{ q'_j \} - [S]^T [\Delta h_{j-1}] \{ w'_{j-1} \} + [[h_{j-1}]] [S]^T - [S]^T [h'_{j-1}] \right\} \{ w_{j-1} \}$$

$$u_j'' = \frac{F_j}{A_j \left(\rho_j - h_{fg} \frac{\partial \Psi}{\partial h} \right)} \quad (54)$$

$$q'_j = \sum_{m \in i} P_H \phi_{im} q_w^{*n+1} \quad (55)$$

Finite-Difference equation for pressure:

Finite difference equations of pressure drop are presented as below equations :

$$\{P_J^{n+1} - P_J^n\} = \{N_J\} \Delta x_J + [R_J] \{w_J^{n+1}\} \Delta x_J \quad (56)$$

$$\{N_J\} = -\left\{K_J (F_J^{n+1})^2\right\} - \{f_J\} - [A_J]^{-1} \left\{\frac{F_J^{n+1} - F_J^n}{\Delta t}\right\} + [B_J] \left\{\frac{\rho_J^{n+1} - \rho_J^n}{\Delta t}\right\}$$

$$[R_J] = [A_J]^{-1} \left[[B_J] [S]^T - [S]^T [U_J^*] \right] \quad (58)$$

$$[B_J] = \left[\frac{\Delta x}{\Delta t} + 2U_J + \Delta x_J K_J A_J (F_J^{n+1} + F_J^n) \right] \quad (59)$$

All of the parameters that have been used in the equations have been introduced in nomenclature Table.

TURBULENT INTERCHANGE

Turbulent interchange is postulated to be associated with turbulent eddies that move between the rod gaps. For the single-phase flow case physics dictates that there is no net exchange of mass between the subchannels. For two phase boiling flows this is not the case given the disparate densities of the liquid and vapor phases. Unlike the diversion crossflow, the turbulent interchange is not obtained from the basic fluid flow equations. Empirical correlations are used instead and are specified outside the basic equation framework. These correlations for two adjacent subchannels i and j that are presented below:

$$w'_{ij} = w'_{ij,g} + w'_{ij,l} \quad (60)$$

$$w'_{ij,g} = V'_{ij} \cdot \rho_{ave,g} \left[(\alpha_i - \alpha_j) - \frac{\alpha_{ave}}{G_{m,i}} (G_{m,i} - G_{m,j}) \right] S_{ij} \quad (61)$$

$$w'_{ij,l} = -V'_{ij} \cdot \rho_{ave,l} \left[(\alpha_i - \alpha_j) - \frac{\alpha_{ave}}{G_{m,i}} (G_{m,i} - G_{m,j}) \right] S_{ij} \quad (62)$$

$$V'_{ij} = J_{ave} (\beta_{ij})_{TP} \quad (63)$$

$$J = \frac{x G_m}{\rho_g} + \frac{(1-x) G_m}{\rho_l} \quad (64)$$

$$G_{ave} = \frac{G_{m,i} A_i + G_{m,j} A_j}{A_i + A_j}, \rho_{ave,g} = \frac{\rho_{g,i} + \rho_{g,j}}{2} \quad (65)$$

$$\rho_{ave,l} = \frac{\rho_{l,i} + \rho_{l,j}}{2}, \alpha_{ave} = \frac{\alpha_i + \alpha_j}{2}, J_{ave} = \frac{J_i + J_j}{2}$$

$$(\beta_{ij})_{TP} = \theta_{TP} \cdot (\beta_{ij})_{SP} \quad (66)$$

$$(\beta_{ij})_{SP} = (0.5)(0.0058) \left(\frac{S_{ij}}{d_{tube}} \right)^{-1.46} \text{Re}_i^{-0.1} \left[1 + \left(\frac{D_{hyd,j}}{D_{hyd,i}} \right)^{1.5} \right] \left(\frac{D_{hyd,i}}{d_{tube}} \right)$$

(67)

$$\theta_{TP} \begin{cases} 1 + (\theta_M - 1) \frac{x}{x_c} & : x < x_c \\ 1 + (\theta_M - 1) \frac{\left[1 - \left(\frac{x}{x_c} \right) \right]}{\left(\frac{x}{x_c} \right) - \left(\frac{x_e}{x_c} \right)} & : x \geq x_c \end{cases}$$

$$\frac{x_0}{x_c} = (0.57) \text{Re}_i^{0.0417} \quad (69)$$

$$\theta_M = 5.0 \quad (70)$$

$$\text{Re}_i = \frac{G_{m,i} \cdot D_{hyd,i}}{\mu_i} \quad (71)$$

$$x_c = \frac{\left[\frac{0.4 \sqrt{9 D_{hyd} \rho_l (\rho_l - \rho_g)}}{G_{m,i}} \right] + 0.6}{\sqrt{\frac{\rho_l}{\rho_g}}} \quad (72)$$

APPLYING SUBCHANNEL GEOMETRY

The flow area shown in the Figure 2 for OTSG must be divided into the some subchannels in order to apply subchannel approach. Figure 4 shows the considered subchannels. There are totally 42 subchannels that can be classified in 3 types. Twenty four of them are triangular form (central parts), 12 of them are rectangular and 6 subchannels are at the corners. Obtained geometry after dividing has one over six symmetry and includes 3 types of subchannels called A, B and C that are shown in Figure 4. Because of symmetry one part is chosen and will be analyzed, so the results can be extended to the same type of subchannels. This part includes 7 subchannels, 7 gaps and 6 tubes.

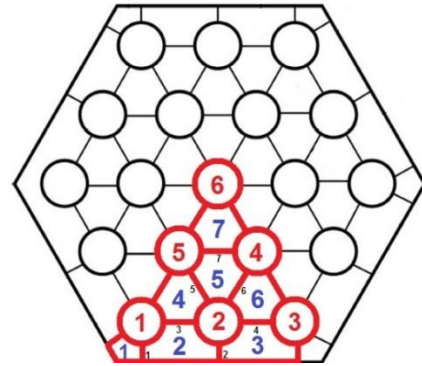


Figure 4 Steam generator cross section, divided into subchannels

RESULTS
SHC results

The algorithm that has been used to calculate primary and secondary side fluid temperature and primary and secondary wall temperature in SHC method is shown in Figure 5:

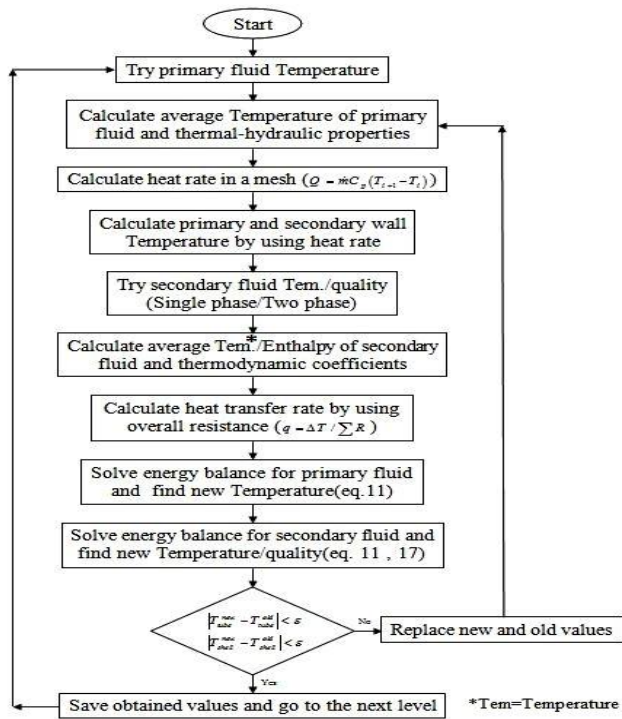


Figure 5Algorithm for calculating primary and secondary fluid and wall temperatures

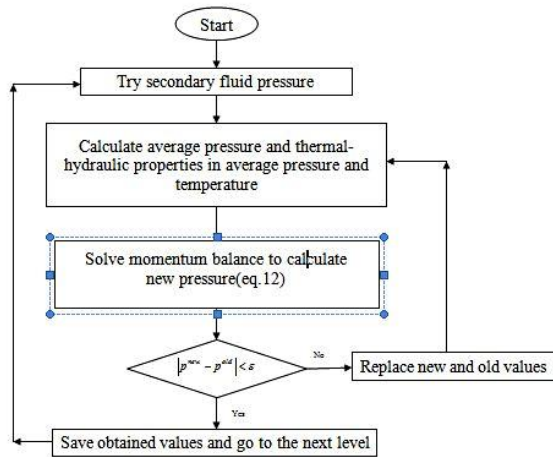


Figure 6Algorithm for calculating primary and secondary side pressure

Calculation of heat transfer from primary side to the secondary side has the high degree of importance and can affect the results. Also the algorithm of pressure drop calculation has been shown in Figure 6. The results have been presented in Figure 7 to 10.

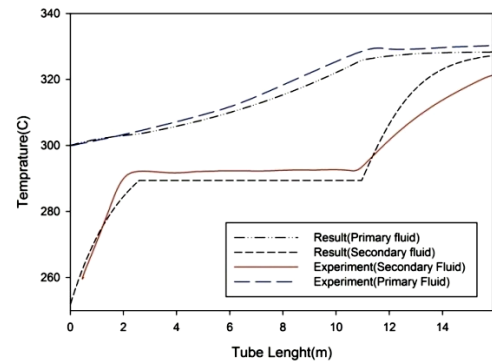


Figure 7Primary and secondary fluid temperatures

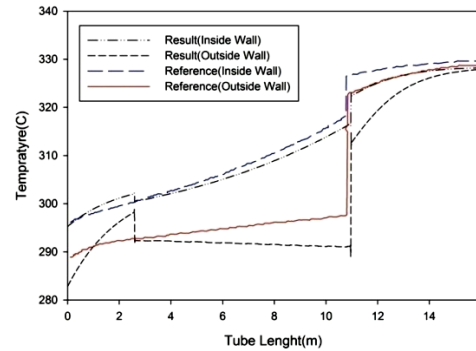


Figure 8Primary and secondary wall temperatures

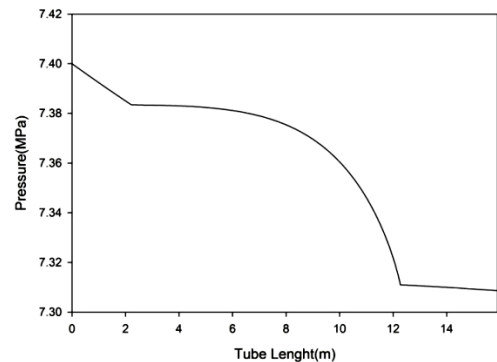


Figure 9Secondary fluid pressure drop

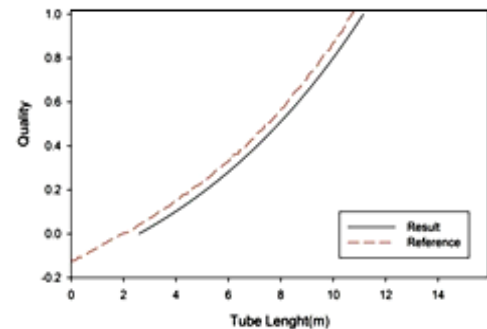


Figure 10 Secondary fluid quality distribution

As can be seen in these figures, as the temperature of primary fluid decreases the temperature of secondary fluid increases. After beginning the boiling, temperature of secondary fluid

remains constant till the quality reaches 1.0 and super heated region begins. Results have been presented for a single heated channel on behalf of the OTSG and have been compared with experimental data [6].

SUBCHANNEL RESULTS

Validation of Subchannel Modeling

Before applying the subchannel modeling on the OTSG, a 9-fuel rod General Electric's laboratory core has been used to validate subchannel modeling. The geometry and boundary condition of this core are shown in Figure 11 and Table 2. The algorithm of calculation in subchannel model is shown in Figure 12.

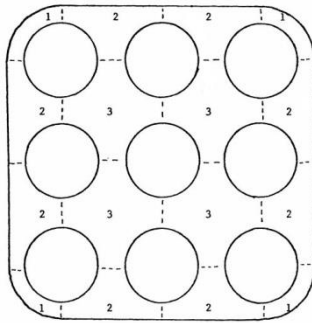


Figure 11- fuel rod GE's laboratory core geometry

Table 2 Boundary Condition for General Electric 9 fuel rod core

Primary fluid output temperature	300 °C
Primary fluid output velocity	5.6 m/s
Primary fluid pressure	15.3 MPa
Secondary fluid input temperature	251.7 °C
Secondary fluid input velocity	0.3 m/s
Secondary fluid pressure	7.4 MPa

Results have been presented in Figure 13 to 15 and compared with the results of THERMIT code. As can be seen on these figures results show a great similarity and the ability of subchannel code has been cleared.

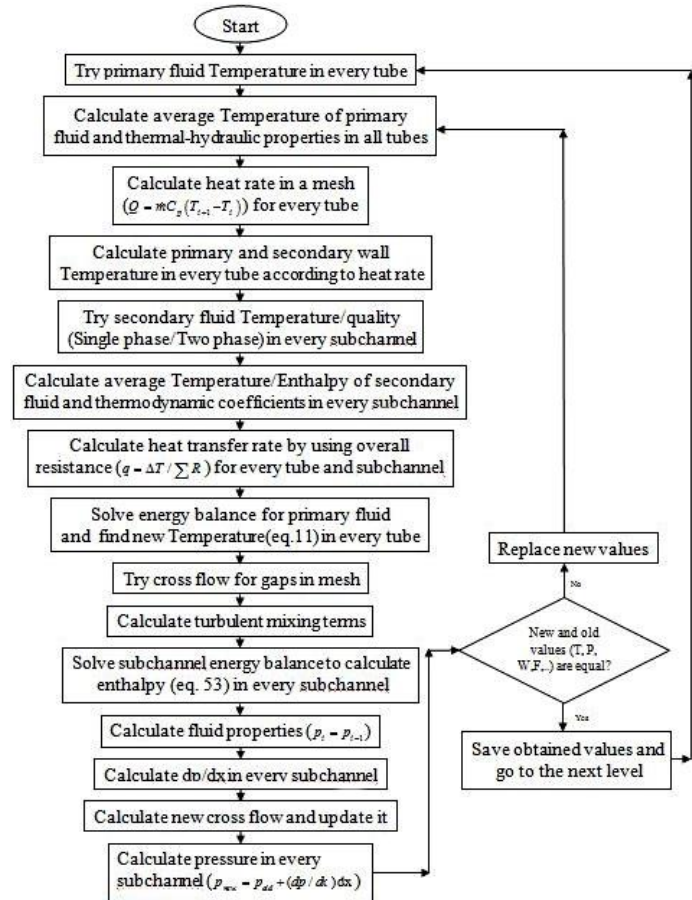


Figure 12 Algorithm used in subchannel approach

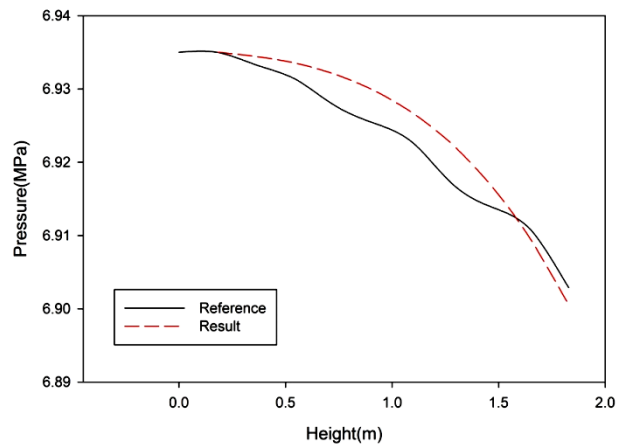


Figure 13 Pressure drop in subchannel type 2 and 3

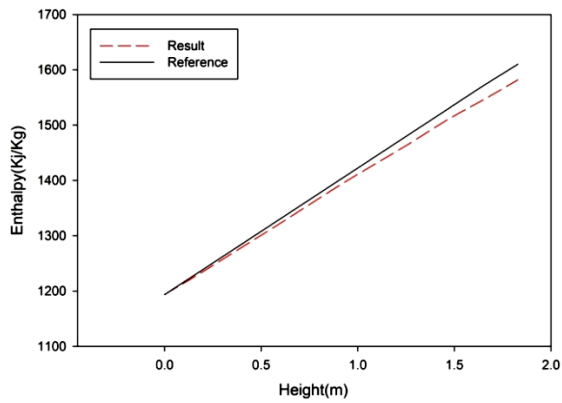


Figure 14 Enthalpy change in subchannel type 3

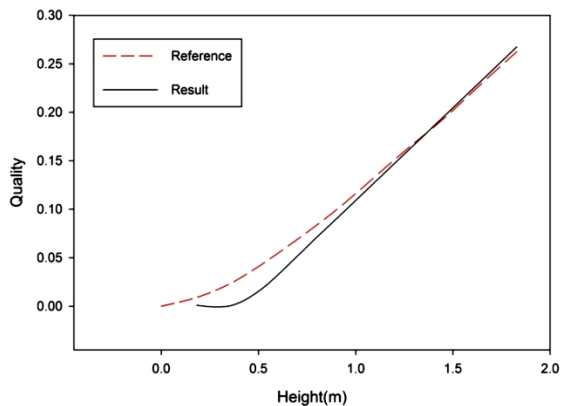


Figure 15 Quality distribution in subchannel type 3

OTSG RESULTS

The first part of algorithm (Figure 14) in modeling of the steam generator (calculating heat transfer from primary fluid to the secondary fluid) is almost same with the SHC method. The most important difference is that heat transfer must be calculated for every given tube that is connected with the specified subchannels. Also the portion of tube that is faced with those subchannels must be considered. The results are presented in Figure 16 to 21 and have been compared with central tube experimental data (experimental data are only available for central tube in reference).

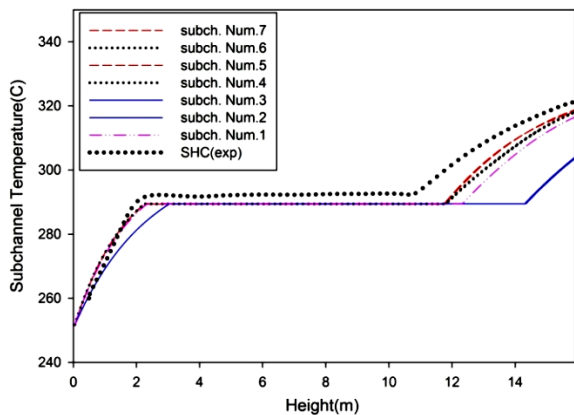


Figure 16 Secondary side temperature for subchannels

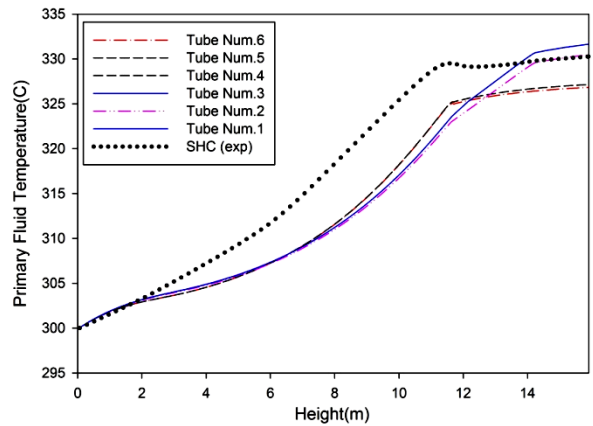


Figure 17 Primary side temperature for tubes

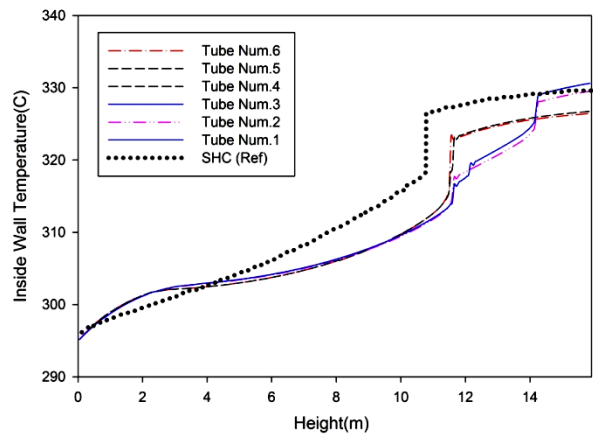


Figure 18 Inside wall temperatures

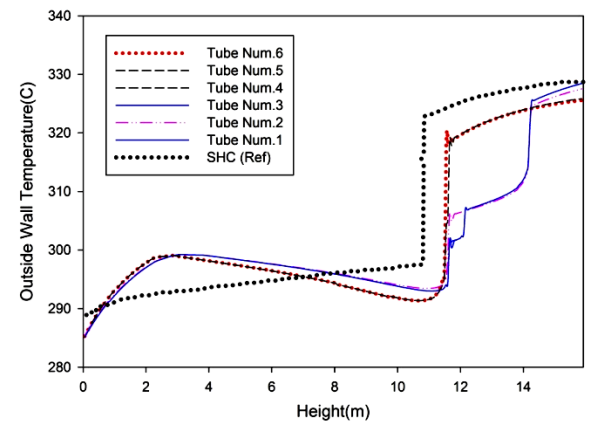


Figure 19 Secondary wall temperatures

As can be seen in these figures, the trend of primary and secondary fluids in tubes and subchannels are same as experimental data. Behavior of the primary and secondary fluids in central tubes and subchannels are very similar to those in experiment. The transition points in these tubes and subchannels are very close to each other, that is because of the similarity of adjacent subchannels that are around central tubes (consider tube number 6 and subchannel number 7, or

tube number 5 and subchannel number 4,5). Going far from central region of shell side which the variety of subchannels around each tube increases, the sharper temperature differences can be seen in figures 18 to 19(consider tube number 1 and subchannel number 1,2,4. or tube number 2 and subchannels number 2,3,4,5,6). Flow pattern in every subchannel is affected by adjacent subchannels.. Finally pressure profile and quality have been shown in Figure 20 and 21.

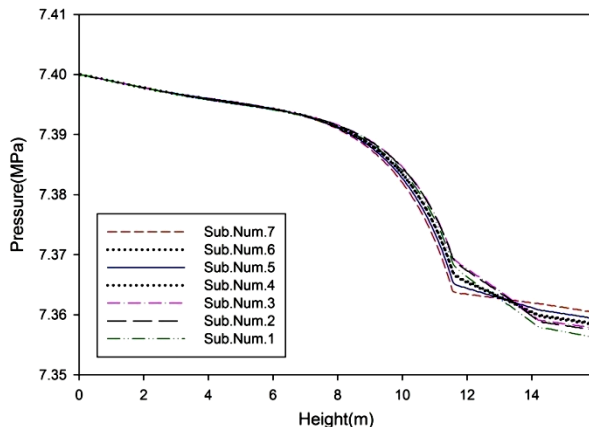


Figure 20 Secondary side pressure drop

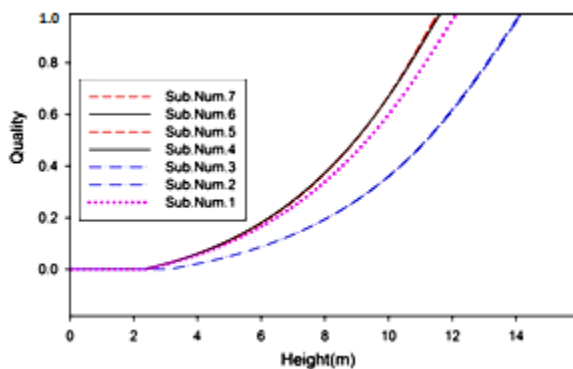


Figure 21 Secondary side quality distribution

As can be seen in Figure 21 two-phase flow has been happened in different height for each subchannel according to its situation.

CONCLUSION

In this study, primary and secondary fluids of Integral Once Through Steam Generator (IEOTSG) is analyzed by Single Heated Channel (SHC) and subchannel approach. The SHC method is the most popular method that has been used by thermal-hydraulic codes and previous researchers that shows unique trend and behaviour for primary and secondary fluids in all tubes and different locations of shell side of OTSG. Using subchannel approach can present a localized profile for each tube and all channels (Figure 16 to 21). It can provide a good platform to see the different regions in each subchannel. Finally comparison of results with experimental data can provide an

appropriate understanding of single heated channel and subchannel approach.

REFERENCES

- [1] SINGHA, A.K. and G. SRIKANTIA, *A Review of Thermal Hydraulic Analysis Methodology for PWR Steam Generators and ATHOS3 Code Applications* Progress in Nuclear Energy, 1991. **Vol. 25, No. 1**: p. pp. 7-70.
- [2] Wang, Z.L., et al., *Numerical study on annular tube once-through steam generator using compressible flow model*. Annals of Nuclear Energy, 2012. **39**: p. 49-55.
- [3] Jingyan, Z., G. Yun, and Z. Zhijian, *Dynamic simulation of once-through steam generator with concentric annuli tube*. Annals of Nuclear Energy, 2012. **50**: p. 158-198.
- [4] Cong, T., et al., *Study on secondary sideflow of steam generator with coupled heat transfer from primary to secondary side*. Applied Thermal Engineering, 2013. **61**: p. 519-530.
- [5] Li, Y., Y. Yang, and B. Sun, *Numerical investigation of thermal-hydraulic characteristics in a steam generator using a coupled primary and secondary side heat transfer model*. Annals of Nuclear Energy, 2013. **55**: p. 258-264.
- [6] Li, H., X. Huang, and L. Zhang, *A lumped parameter dynamic model of the helical coiled once-through steam generator with movable boundaries*. Nuclear Engineering and Design, 2008. **238**: p. 1657-1663.
- [7] Osakabe, M., *Thermal-Hydraulic Study of Integrated Steam Generator in PWR* Journal of Nuclear Science and Technology, 1988. **26(2)**: p. 286~294.
- [8] Sun, F., G. Xia, and J. Sun, *Simulation research on dynamic characteristics of new once-through steam generator*. Applied Science and Technology, 2005. **32**: p. 49-52.
- [9] Sun, F., G. Xia, and J. Sun, *Simulation research on dynamic characteristics of new once-through steam generator*. Applied Science and Technology, 2005. **32**: p. 49-52.
- [10] J.E.Kelly, S.P.Kao, and M.S.Kazimi, *User's Guide for THERMIT-2 : A Version of THERMIT for Both Core-Wide and Subchannel Analysis of Light Water Reactors*, MIT, Editor. 1981, MIT Energy Laboratory Electric Utility Program Report No. MIT-EL-81-029.
- [11] COLLIER, J.G. and J.R. THOME, *Convective Boiling and Condensation* 1994, Walton Street, Oxford OX2 6DP: CLARENDON PRESS · OXFORD.
- [12] Kazimi, M.S. and N.E. Todreas, *NUCLEAR SYSTEMS 1 Elements of Thermal Hydraulic Design*. 2 ed. 1990, UNITED STATES: Taylor & Francis.
- [13] *COBRA-FLX: A Core Thermal-Hydraulic Analysis Code Topical Report*. 0 ed. ANP-10311NP. 2010.